



Deposited via The University of Sheffield.

White Rose Research Online URL for this paper:

<https://eprints.whiterose.ac.uk/id/eprint/183080/>

Version: Published Version

Article:

Yang, H., Ye, Y., Liang, K. et al. (2021) Energy efficiency maximization for symbiotic radio networks with multiple backscatter devices. IEEE Open Journal of the Communications Society, 2. pp. 1431-1444. ISSN: 2644-125X

<https://doi.org/10.1109/ojcoms.2021.3090836>

Reuse

This article is distributed under the terms of the Creative Commons Attribution (CC BY) licence. This licence allows you to distribute, remix, tweak, and build upon the work, even commercially, as long as you credit the authors for the original work. More information and the full terms of the licence here:

<https://creativecommons.org/licenses/>

Takedown

If you consider content in White Rose Research Online to be in breach of UK law, please notify us by emailing eprints@whiterose.ac.uk including the URL of the record and the reason for the withdrawal request.

Energy Efficiency Maximization for Symbiotic Radio Networks With Multiple Backscatter Devices

HAOHANG YANG¹, YINGHUI YE² (Member, IEEE), KAI LIANG³,
AND XIAOLI CHU¹ (Senior Member, IEEE)
(Invited Paper)

¹Department of Electronic and Electrical Engineering, University of Sheffield, Sheffield S1 4ET, U.K.

²Shaanxi Key Laboratory of Information Communication Network and Security, Xi'an University of Posts and Telecommunications, Xi'an 710121, China

³State Key Laboratory of Integrated Service Networks, Xidian University, Xi'an 710071, China

CORRESPONDING AUTHOR: X. CHU (e-mail: x.chu@sheffield.ac.uk)

This work was supported in part by the European Union Horizon 2020 Research and Innovation Program under Grant 734798; in part by the National Key R&D Program of China under Grant 2019YFE0113200; in part by the National Natural Science Foundation of China under Grant 61901317; in part by the Fundamental Research Funds for the Central Universities under Grant JB190104; in part by the Joint Education Project between China and Central–Eastern European Countries under Grant 202005; in part by the 111 Project under Grant B08038; in part by the Natural Science Foundation of Shaanxi Province under Grant 2021JQ-713; and in part by the Scientific Research Program Funded by Shaanxi Provincial Education Department under Grant 21JK0914.

ABSTRACT Driven by the limited radio spectrum resources and the high energy consumption of wireless devices, symbiotic radio (SR) has recently been proposed to support passive Internet-of-Things (IoT) networks, where a primary transmitter (PT) transmits information to a primary reader (PR), while passive backscatter devices (BDs) modulate their own information on the received primary signal and backscatter the modulated signal to the same PR by adjusting their reflection coefficients. Existing works on SR have mainly studied the case of a single BD while without considering the BD's energy harvesting (EH) ability. In this paper, we aim to maximize the energy efficiency (EE) of an SR system that includes multiple BDs each being able to harvest energy while backscattering, by jointly optimizing the PT transmission power and the BDs' reflection coefficients and time division multiple access (TDMA) time slot durations for both the parasitic SR (PSR) and commensal SR (CSR) cases. To solve the formulated non-convex optimization problems, we propose a Dinkelbach-based iterative algorithm that builds on the block coordinated decent (BCD) method and the successive convex programming (SCP) technique. Simulation results show that the proposed algorithm converges fast, and the system EE is maximized when the BD that can provide the highest EE is allocated the maximum allowed time for backscattering while guaranteeing the throughput requirements for both the primary link and the other backscatter links.

INDEX TERMS Backscatter communication, energy efficiency, resource allocation, symbiotic radio, wireless power transfer.

I. INTRODUCTION

IT IS predicted that the Internet of Things (IoT) devices will be over 80 billion worldwide by 2030 [1], putting huge pressure on wireless networks concerning the limited radio spectrum resources and soaring energy consumption. In order to support massive IoT connections, cognitive radio (CR) technology has been employed to let IoT devices (as secondary transmitters (STs)) share the same spectrum with incumbent primary transmitters (PTs) [2], [3], [4], [5].

However, the energy efficiency (EE) of a CR system is limited by the energy-consuming active radio frequency (RF) components used in the STs [2], [6].

Different from active RF transmissions, backscatter communications (BackCom) [7], [8], [9], [10], [11], [12] allow a backscatter device (BD) to modulate its own information on the incident RF signal transmitted by a PT and backscatter the modulated signal to the desired receiver by adjusting its reflection coefficient [13], [14], [15], while harvesting

energy from the incident RF signal to cover its circuit power consumption [11]. Thus, the energy consumption of passive BackCom is significantly reduced as compared with active transmissions in CR. However, since the BDs have no knowledge of the information transmitted by the PT, the EE of BackCom will be limited by the strong interference caused by the PT [6].

To exploit the synergy between CR and BackCom, symbiotic radio (SR) has been proposed recently [6], where the PT and the primary receiver (PR) are designed to support both the primary and BackCom transmissions, and has attracted a lot of research interest. Depending on whether the BD symbol period is equal to or much longer than the PT symbol period, SR is classified into parasitic SR (PSR) and commensal SR (CSR), respectively [2]. The authors in [2] jointly optimized the transmission power and beamforming vectors of a multi-antenna PT to maximize the weighted sum-rate and minimize the transmission power separately in an SR system. In [16], the weighted sum-rate of an SR network was maximized through optimizing the PT transmission power and the BD reflection coefficient under either a long-term or short-term PT transmission power constraint. The authors in [17] derived the expressions of the outage probability and the ergodic rate for an SR system, where the base station transmits information to two cellular users and a BD backscatters its information to one of the two cellular users, and analyzed the corresponding diversity orders. In [18], the PT transmission power was minimized by jointly designing the beamforming vector at the PT and the power splitting factor at the full-duplex BD, while guaranteeing the minimum BD rate requirement. The authors in [19] maximized the system EE subject to the throughput requirements of the direct and backscatter links as well as the PT transmit power constraint, by optimizing the PT beamforming vectors in an SR system with a finite block length backscatter link. Nevertheless, the above works considered only a single BD while ignoring the energy harvesting (EH) ability of the BD.

In this paper, we investigate the EE maximization problem of an SR system with multiple BDs, each being able to harvest energy from the incident primary signal to support their circuit power consumption. Our main contributions are summarized as follows.

- We propose an SR system, where following the time division multiple access (TDMA) protocol but allocating a BD-specific time slot duration to each BD, multiple BDs take turn to modulate their own information on the incident primary signal and backscatter the modulated signal to the PR, while harvesting energy from the incident primary signal to support their circuit operation.
- We formulate an optimization problem to maximize the EE of the SR system by jointly optimizing the PT transmission power and the BDs' reflection coefficients and TDMA time slot durations for both the PSR and CSR cases.

- Due to multiple coupled variables in the objective function and the constraints, the formulated problem is non-convex and is hard to solve directly. To solve the problem, in the PSR case, we first introduce auxiliary variables and utilize the Dinkelbach-based method to transform the original problem from a fraction form into a subtraction form, then employ a block coordinate decent (BCD) method in conjunction with a successive convex programming (SCP) technique to transform the objective function into a convex function, and obtain the sub-optimal solutions of the PT transmission power, the BDs' reflection coefficients, or the BDs' time slot durations, given the other variables by using the interior point method. The closed-form expression of the sub-optimal reflection coefficients is derived by employing the Lagrange dual method. In the case of CSR, as the system EE is a monotonically increasing function of the BDs' reflection coefficients, we first obtain the globally optimal reflection coefficients. Then, employing techniques similar to the PSR case but without using the BCD method, we obtain the sub-optimal solutions of the PT transmission power and the BDs' time slot durations, and derive the closed-form expressions of the optimal reflection coefficients and the sub-optimal PT transmission power. Based on the above obtained solutions, we propose a Dinkelbach based iterative algorithm to solve the formulated problems in the PSR and CSR cases.
- The convergence and computational complexity of the proposed algorithm are analyzed and verified by simulation. The simulation results show that the proposed algorithm converges very fast and the system EE is maximized when the BD that can contribute the most toward the system EE is allocated the maximum allowed time to backscatter its information to the PR while the other BDs' throughputs being kept at the minimum required level. This best BD is determined by the optimized PT transmission power in the corresponding time slot.

The rest of the paper is organized as follows. The system model is presented in Section II. In Sections III and IV, the system EE maximization problem is formulated and solved, respectively. Section V presents the Dinkelbach based iterative algorithm for maximizing the system EE. Section VI analyzes the convergence and the computational complexity of the proposed algorithm. In Section VII, the simulation results are presented. Section VIII concludes the paper.

II. SYSTEM MODEL

In this section, we introduce the SR network with multiple BDs, present the throughout analysis for both the PSR and CSR cases, and define the system EE of the network.

A. NETWORK MODEL

As shown in Fig. 1, the SR network consists of a PT, a PR and M BDs, where each BD $i \in \mathcal{M} = \{1, \dots, M\}$ is equipped with a single antenna, an EH circuit and a passive

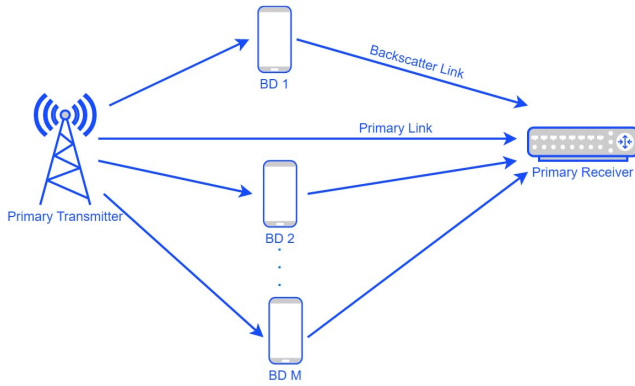


FIGURE 1. An SR Network.

backscatter circuit.¹ The PT transmits its information to the PR through a direct link, meanwhile BD i modulates its own information on the incident primary signal from the PT and backscatters the modulated signal to the PR by adjusting its reflection coefficient. The BDs share the same RF channel with the primary link. The mutual interference among the BDs during BackCom can be avoided by employing TDMA, where a time block T is divided into M time slots for the M BDs, i.e., $\sum_{i=1}^M t_i \leq T$, and t_i is the duration of the i th time slot allocated to BD i for BackCom and EH at the same time, while all the other BDs staying idle. Assuming that there is no internal power source or energy storage in the BDs, the harvested energy during BackCom is used up for BD circuit operation and cannot be stored [14].

We use a block flat-fading channel model, where the channel parameters stay constant during each time block T [2]. The channel power gain of the direct link from the PT to the PR is denoted by $h^{t,r} = (d^{t,r})^{-\alpha} \mu^{t,r}$, where $d^{t,r}$, α and $\mu^{t,r}$ are the distance, the path-loss exponent and the Rayleigh fading power gain of the link from the PT to the PR, respectively. We denote the channel power gain from the PT to BD i and that from BD i to the PR by $h_i^{t,b} = (d_i^{t,b})^{-\alpha} \mu_i^{t,b}$ and $h_i^{b,r} = (d_i^{b,r})^{-\alpha} \mu_i^{b,r}$, respectively, where $d_i^{t,b}$ and $d_i^{b,r}$ are the distance from the PT to BD i and that from BD i to the PR, respectively, $\mu_i^{t,b}$ and $\mu_i^{b,r}$ are the Rayleigh fading power gain from the PT to BD i and that from BD i to the PR, respectively.

The amount of energy harvested by BD i during the i th time slot is given by

$$EH_i = t_i P_i h_i^{t,b} (1 - z_i) \eta, \quad (1)$$

where P_i and z_i are the PT transmission power and the reflection coefficient of BD i in the i th time slot, respectively, and η represents the energy conversion efficiency of the EH circuit. We ignore the energy harvested from the thermal

1. BackCom systems can be mainly classified into passive systems and semi-passive systems, where the key benefits of a passive BD without any internal energy storage are its low cost and small size [14], [20]. In this paper, we consider passive BDs where the energy is only harvested for covering circuit power consumption and is not stored in the BDs.

noise as it is much lower than the RF energy [15], [21]. Accordingly, the total amount of energy harvested by all the BDs in a time block T is given by $EH_{sum} = \sum_{i=1}^M EH_i$.

B. THROUGHPUT ANALYSIS

Denote the primary signal transmitted from the PT by $s(n)$ with symbol period of T_s and the i th BD's signal by $c_i(l)$ with symbol period of T_c , where n and l are the indices of symbols of the primary signal and the BackCom signal, respectively. The symbol periods T_s and T_c are much shorter than t_i , $i \in \mathcal{M}$. It is assumed that $s(n)$ and $c_i(l)$ follow independent standard circularly symmetric complex Gaussian distribution $\mathcal{CN}(0, 1)$. Thus, the backscattered signal from BD i is given by $\sqrt{z_i} c_i(l)$, where $z_i \in [0, 1]$ is the reflection coefficient of BD i . Following [2], we consider two cases of SR, one is the PSR with $T_s = T_c$, and the other is the CSR with $T_c = NT_s$, where $N \gg 1$ is a positive integer, i.e., the symbol period of the BackCom is much longer than that of the primary transmission. In the following, we will analyze the throughputs of the primary link and BackCom links for the two cases separately.

1) PSR

Since $T_s = T_c$, we assume that $l = n$ and the received signal at the PR for the n th primary symbol in the i th time slot is given by

$$y(n)^{(1)} = \sqrt{P_i} h^{t,r} s(n) + \sqrt{P_i z_i h_i^{t,b} h_i^{b,r}} s(n) c_i(n) + k(n), \quad (2)$$

where $k(n)$ is the additive white Gaussian noise (AWGN) with zero mean and power σ^2 .

According to (2), the received signal from BD i is weaker than that from the PT. Therefore, the PR can utilize the successive-interference-cancellation (SIC) technique to decode the primary signal $s(n)$ first, then remove $s(n)$ from the received signal $y(n)^{(1)}$, and detect the BackCom signal $c_i(n)$. Since the symbol rates of $s(n)$ and $c_i(n)$ are the same in the PSR case, $c_i(n)$ is regarded as interference when decoding $s(n)$. As we can see from the second term on the right-hand side of (2), the interference is the product of two complex Gaussian signals $s(n)$ and $c_i(n)$, and thus follow a non-Gaussian distribution. The lower bound of the PT-PR link throughput (bits) in a time block is given by [2]

$$R^{s(1)} = \sum_{i=1}^M W t_i \log_2 \left(1 + \frac{P_i h^{t,r}}{P_i z_i h_i^{t,b} h_i^{b,r} + \sigma^2} \right), \quad (3)$$

where W is the channel bandwidth.

Assuming that the primary signal is perfectly removed from $y(n)^{(1)}$ by SIC [2], [16], [17], [18], [19], we have

$$y'(n)^{(1)} = \sqrt{P_i z_i h_i^{t,b} h_i^{b,r}} s(n) c_i(n) + k(n). \quad (4)$$

Regarding $s(n)$ as a random channel component imposed on $c_i(n)$, the throughput of BD i in the i th time slot is given by [22]

$$R_i^{c(1)} = W t_i E_s \left[\log_2 \left(1 + \frac{P_i z_i h_i^{t,b} h_i^{b,r} |s(n)|^2}{\sigma^2} \right) \right], \quad (5)$$

where $|s(n)|^2$ follows the exponential distribution with a unit rate.

2) CSR

Since $T_c = NT_s$, $N \gg 1$, the BackCom symbol $c_i(l)$ spans N primary symbol periods for $n = 1, \dots, N$. Accordingly, the received signal at the PR for the n th primary symbol is written as

$$y(n)^{(2)} = \sqrt{P_i h^{t,r}} s(n) + \sqrt{P_i z_i h_i^{t,b} h_i^{b,r}} s(n) c_i(l) + k(n), \quad (6)$$

where $c_i(l)$ can be regarded as a constant coefficient for decoding $s(n)$, $n = 1, \dots, N$. For given $c_i(l)$, the throughput of the PT-PR link in a time block is given by

$$R^{s(2)'} = \sum_{i=1}^M W t_i \mathbb{E}_{c_i} [\log_2(1 + \gamma_i^s)], \quad (7)$$

where $\gamma_i^s = \frac{P_i h^{t,r} + P_i z_i h_i^{t,b} h_i^{b,r} [c_i(l)]^2}{\sigma^2}$ is the signal-to-noise ratio (SNR).

Lemma 1: γ_i^s follows a noncentral chi-square distribution χ^2 with the freedom of 2, and its probability density function (PDF) is given by

$$f_i(x) = \frac{1}{2\theta_i} e^{\left(-\frac{x+\lambda_i}{2\theta_i}\right)} I_0\left(\frac{\sqrt{x\lambda_i}}{\theta_i}\right) \quad (8)$$

where the noncentrality parameter $\lambda_i = \frac{P_i h^{t,r}}{\sigma^2}$, the Gaussian variance parameter $\theta_i = \frac{P_i z_i h_i^{t,b} h_i^{b,r}}{2\sigma^2}$, and $I_0(\cdot)$ is a modified Bessel function of the first kind and is given by

$$I_0(v) = \sum_{m=0}^{\infty} \frac{1}{m! \Gamma(m+1)} \left(\frac{v}{2}\right)^{2m}. \quad (9)$$

Based on (7), the expected throughput of the PT-PR link in a time block over all possible values of $c_i(l)$ is given by

$$R^{s(2)'} = \sum_{i=1}^M W t_i \int_0^{+\infty} \log_2(1+x) f_i(x) dx. \quad (10)$$

Following [2], [16], [17], [18], [19], when $\gamma_i^s \rightarrow +\infty$, the expected throughput of the PT-PR link in a time block is given by

$$R^{s(2)} = \sum_{i=1}^M W t_i \left[\log_2\left(\frac{P_i h^{t,r}}{\sigma^2}\right) - \text{Ei}\left(-\frac{h^{t,r}}{z_i h_i^{t,b} h_i^{b,r}}\right) \log_2 e \right], \quad (11)$$

where $\text{Ei}(x) \triangleq \int_{-\infty}^x \frac{1}{u} e^u du$.

Assuming that the primary signal is perfectly removed from $y(n)^{(2)}$ via maximum-likelihood (ML) detection [23], for $n = 1, \dots, N$, we have

$$y'(n)^{(2)} = \sqrt{P_i z_i h_i^{t,b} h_i^{b,r}} s(n) c_i(l) + k(n). \quad (12)$$

Since $E|s(n)|^2 = 1$, the symbol $c_i(l)$ can be decoded by performing maximal ratio combining (MRC) of $y'(n)^{(2)}$, $n = 1, \dots, N$, received in N consecutive primary symbol periods,

and the throughput of BD i in the i th time slot can be approximately calculated as [2], [16], [17], [18], [19]

$$R_i^{c(2)} = W t_i \frac{1}{N} \log_2 \left(1 + \frac{N P_i z_i h_i^{t,b} h_i^{b,r}}{\sigma^2} \right). \quad (13)$$

C. SYSTEM ENERGY EFFICIENCY

The system EE of the SR network is defined as the ratio of the total throughput of all links to the total energy consumption of the network in a time block [24], [25], [26], [27]. Letting R_{sum}^{PSR} and R_{sum}^{CSR} denote the total throughput of the network for the PSR and the CSR, respectively, we have

$$R_{sum}^{PSR} = R^{s(1)} + \sum_{i=1}^M R_i^{c(1)}, \quad (14)$$

$$R_{sum}^{CSR} = R^{s(2)} + \sum_{i=1}^M R_i^{c(2)}. \quad (15)$$

The total energy consumption of the SR network in a time block is given by

$$EC_{sum} = \sum_{i=1}^M t_i (P_i + P_{cir}^{BD} + P_{cir}^{TR}), \quad (16)$$

where P_{cir}^{BD} and P_{cir}^{TR} represent the circuit power consumption of a BD and that of the PT and PR in total, respectively.

Thus, the system EE in the cases of PSR and CSR is given respectively by

$$EE^{PSR} = \frac{R_{sum}^{PSR}}{EC_{sum} - \min(EH_{sum}, \sum_{i=1}^M t_i P_{cir}^{BD})}, \quad (17)$$

$$EE^{CSR} = \frac{R_{sum}^{CSR}}{EC_{sum} - \min(EH_{sum}, \sum_{i=1}^M t_i P_{cir}^{BD})}, \quad (18)$$

where $\min(EH_{sum}, TP_{cir}^{BD})$ in the denominator on the right-hand side indicates that any excessive energy harvested by BDs will not contribute to a higher system EE, because the BDs do not have any built-in energy storage.

III. PSR SYSTEM ENERGY EFFICIENCY MAXIMIZATION

In this section, we first formulate the system EE maximization problem for the PSR case, then transform the problem into a more tractable form and propose a Dinkelbach-based iterative algorithm to solve it.

A. PROBLEM FORMULATION

We aim to maximize the system EE of the SR network by jointly optimizing the PT transmission power P_i , and BDs' TDMA time slot duration t_i and reflection coefficients z_i , $i \in \mathcal{M}$. Accordingly, the optimization problem is formulated as

$$\begin{aligned} P_1 : \quad & \max_{\{P_i, t_i, z_i\}} EE^{PSR} \\ \text{s.t.} \quad & C1 : 0 \leq P_i \leq P_{\max}, \quad \forall i; \\ & C2 : 0 \leq z_i \leq 1, \quad \forall i; \end{aligned}$$

$$\begin{aligned}
 C3 : t_i &\geq 0, \sum_{i=1}^M t_i \leq T, \forall i; \\
 C4 : R^{s(1)} &\geq R_{\min}^s, R_i^{c(1)} \geq R_{\min}^c, \forall i; \\
 C5 : EH_i &\geq t_i P_{cir}^{BD}, \forall i,
 \end{aligned} \tag{19}$$

where P_{\max} is the maximum transmission power of PT, and R_{\min}^s and R_{\min}^c are the minimum required throughput of the primary link and a backscatter link, respectively; C1 and C2 specify the value ranges of the PT transmission power and BDs' reflection coefficients, respectively; C3 constrains the sum duration of all BDs' time slots in a time block; C4 guarantees the minimum throughput requirements for the primary link and the backscatter links and C5 requires that the harvested energy of each BD should exceed its circuit energy consumption.

We can see that \mathbf{P}_1 contains a fractional objective function with multiple variables coupled in it and in the constraints. As it is extremely difficult to solve \mathbf{P}_1 directly, we will first transform it into a more tractable form.

B. PROBLEM TRANSFORMATION

Assuming that the harvested energy of each BD is sufficient to cover its circuit power consumption while any excessive harvested energy cannot be stored, letting $A_i = h_i^{t,b} h_i^{r,b}$ and introducing an auxiliary variable $L_i = P_i z_i t_i$, we transform \mathbf{P}_1 as

$$\begin{aligned}
 \mathbf{P}_2 : \\
 \max_{\{P_i, t_i, L_i\}} W & \frac{\sum_{i=1}^M t_i \log_2 \left(1 + \frac{P_i h_i^{t,r}}{A_i \frac{L_i}{t_i} + \sigma^2} \right) + \sum_{i=1}^M t_i \mathbb{E}_s \left[\log_2 \left(1 + \frac{A_i L_i |s(n)|^2}{t_i \sigma^2} \right) \right]}{\sum_{i=1}^M t_i (P_i + P_{cir}^{TR})} \\
 \text{s.t. } C1, C3; \\
 C2-1 : 0 &\leq L_i \leq t_i P_i, \forall i; \\
 C4-1 : R^{s(1)'} &\geq R_{\min}^s, R_i^{c(1)'} \geq R_{\min}^c, \forall i; \\
 C5-1 : t_i h_i^{t,b} &\left(P_i - \frac{L_i}{t_i} \right) \eta \geq t_i P_{cir}^{BD}, \forall i,
 \end{aligned} \tag{20}$$

where $R^{s(1)'} = \sum_{i=1}^M W t_i \log_2 \left(1 + \frac{P_i h_i^{t,r}}{A_i \frac{L_i}{t_i} + \sigma^2} \right)$, $R_i^{c(1)'} = W t_i \mathbb{E}_s \left[\log_2 \left(1 + \frac{A_i L_i |s(n)|^2}{t_i \sigma^2} \right) \right]$.

In order to make \mathbf{P}_2 more tractable, we use the Dinkelbach-based method [28], [29], [30] to firstly transform the objective function in \mathbf{P}_2 from a fraction form into a subtraction form. Then, the maximum system EE, denoted by Q^* , can be achieved if and only if the following equation is satisfied,

$$\begin{aligned}
 \max_{\{P_i, t_i, L_i\}} R^{s(1)'} + \sum_{i=1}^M R_i^{c(1)'} - Q \sum_{i=1}^M t_i (P_i + P_{cir}^{TR}) \\
 = R^{s(1)'} + \sum_{i=1}^M R_i^{c(1)'} - Q^* \sum_{i=1}^M t_i (P_i^* + P_{cir}^{TR}) = 0,
 \end{aligned} \tag{21}$$

where $R^{s(1)'*}$, $R_i^{c(1)'*}$, t_i^* and P_i^* are the optimal value of the throughput of the PT-PR link, the throughput for BD i in

the i th time slot, the TDMA time slot duration and the PT transmit power, respectively.

According to (21), \mathbf{P}_2 is further transformed into

$$\begin{aligned}
 \mathbf{P}_3 : \max_{\{P_i, t_i, L_i\}} R^{s(1)'} + \sum_{i=1}^M R_i^{c(1)'} - Q \sum_{i=1}^M t_i (P_i + P_{cir}^{TR}) \\
 \text{s.t. } C1, C2 - 1, C3, C4 - 1, C5 - 1.
 \end{aligned} \tag{22}$$

C. PROBLEM SOLUTION

We note that \mathbf{P}_3 is still non-convex due to multiple coupled variables. To this end, we propose a BCD method to solve \mathbf{P}_3 alternatively, i.e., to optimize L_i, t_i under a fixed P_i and then optimize P_i under the updated L_i, t_i .

For a fixed P_i , we apply the successive convex programming (SCP) technique on $R^{s(1)'}$ to transform it into a convex form and successively maximize a lower bound of the objective function of \mathbf{P}_3 in an iterative manner based on the following lemma.

Lemma 2: For any given $X_i^{(j)} = \frac{L_i^{(j)}}{t_i^{(j)}}$, $j > 0$, where $L_i^{(j)}$ and $t_i^{(j)}$ denote the obtained values after the j th iteration, we have

$$R^{s(1)'}(X_i) \geq R^{s(1)'}(X_i^{(j)}), \forall i, \tag{23}$$

where

$$\begin{aligned}
 R^{s(1)'}(X_i^{(j)}) = W t_i \left[\log_2 \left(1 + \frac{P_i h_i^{t,r}}{A_i X_i^{(j)} + \sigma^2} \right) - \frac{P_i h_i^{t,r} A_i \log_2 e}{(A_i X_i^{(j)} + \sigma^2 + P_i h_i^{t,r})(A_i X_i^{(j)} + \sigma^2)} \right. \\
 \left. \times (X_i - X_i^{(j)}) \right],
 \end{aligned} \tag{24}$$

and the equalities only hold when $X_i = X_i^{(j)}$.

Proof: Please see Appendix A. ■

By substituting (24) into (22) and after some manipulations, \mathbf{P}_3 is equivalently formulated as

$$\begin{aligned}
 \mathbf{P}_{3.1} : \\
 \{t_i^*, L_i^*\} = F_1 = \arg \max_{\{t_i, L_i\}} \sum_{i=1}^M W \\
 \times \left[t_i \log_2 \left(1 + \frac{P_i h_i^{t,r}}{A_i X_i^{(j)} + \sigma^2} \right) - \frac{P_i h_i^{t,r} A_i \log_2 e}{(A_i X_i^{(j)} + \sigma^2 + P_i h_i^{t,r})(A_i X_i^{(j)} + \sigma^2)} (L_i - t_i X_i^{(j)}) \right] \\
 + \sum_{i=1}^M W t_i \\
 \mathbb{E}_s \left[\log_2 \left(1 + \frac{A_i L_i |s(n)|^2}{t_i \sigma^2} \right) \right] - Q \sum_{i=1}^M t_i (P_i + P_{cir}^{TR}) \\
 \text{s.t. } C2 - 1, C3, C5 - 1;
 \end{aligned}$$

$$C4 - 2 : R^{s(1)'}(X_i^{(j)}) \geq R_{\min}^s, R_i^{c(1)'} \geq R_{\min}^c, \forall i. \quad (25)$$

It is easy to verify that the first and third terms of the objective function in $\mathbf{P}_{3.1}$ are linear with respect to L_i and t_i , and the second term of the objective function is a standard log-form convex function. Thus, $\mathbf{P}_{3.1}$ is jointly convex with respect to L_i and t_i , and it can be efficiently solved by standard convex optimization methods, e.g., the interior point method [31], the detail of which is omitted for saving space.

For the obtained L_i and t_i , \mathbf{P}_3 is equivalently formulated as

$$\begin{aligned} P_{3.2} : F_2 = \max_{\{P_i\}} & R^{s(1)'} + \sum_{i=1}^M R_i^{c(1)'} - Q \sum_{i=1}^M t_i (P_i + P_{cir}^{TR}) \\ \text{s.t.} & C1, C2 - 1, C4 - 1, C5 - 1. \end{aligned} \quad (26)$$

It is easy to verify that $\mathbf{P}_{3.2}$ is convex with respect to P_i since the first and third terms of the objective function are convex and linear with respect to P_i , respectively, while the second term of the objective function is constant for the obtained L_i and t_i . Thus, we can easily solve $\mathbf{P}_{3.2}$ by applying the interior point method.

Lemma 3: To gain more insights, we derive the closed form expressions of the optimal reflection coefficient z_i and the optimal PT transmission power P_i by employing the Lagrange dual method as follows.

$$\begin{aligned} z_i^* &= \frac{1}{P_i} \\ &\times \left[\frac{(1 + \delta_i) \log_2 e}{\mu_i + \varepsilon_i + (1 + \beta) \frac{P_i h^{t,r} A_i \log_2 e}{(A_i X_i^{(j)} + \sigma^2 + P_i h^{t,r}) (A_i X_i^{(j)} + \sigma^2)}} - \frac{\sigma^2}{A_i} \right], \end{aligned} \quad (27)$$

$$P_i^* = \frac{(1 + \beta) \log_2 e}{Q + \frac{\mu_i - \varepsilon_i}{t_i}} - \frac{A_i X_i + \sigma^2}{h^{t,r}}, \quad (28)$$

where $\beta, \delta_i, \mu_i, \varepsilon_i$ are the Lagrange multipliers associated with C4-1, C2-1 and C5-1, respectively.

Proof: Please see Appendix B. \blacksquare

Remark 1: As we can see in (27), the optimal reflection coefficient is lower with higher PT transmission power, indicating that the EE of the primary link dominates the system EE. This can be explained as follows. Increasing the PT transmission power will lead to higher interference power from the backscatter links to the primary link. Since the EE of the primary link dominates the system EE, the system EE can be increased by the BDs reducing their reflection coefficients so as to reduce their interference to the primary link and to increase the primary link EE. According to (28), the optimal PT transmission power in a time slot increases with a better channel condition of the primary link, i.e., $h^{t,r}$, as well as a longer duration of the time slot, i.e., t_i . The above insights will be verified by simulations.

IV. CSR SYSTEM ENERGY EFFICIENCY MAXIMIZATION

In this section, we first formulate the system EE maximization problem for the CSR network, then transform the problem into a more tractable form and propose a Dinkelbach-based iterative algorithm to solve it.

A. PROBLEM FORMULATION

Similar to the PSR case, the system EE maximization for the CSR case is formulated as

$$\begin{aligned} P_4 : \max_{\{P_i, t_i, z_i\}} & EE^{CSR} \\ \text{s.t.} & C1, C2, C3, C5; \\ & C4 - 3 : R^{s(2)} \geq R_{\min}^s, R_i^{c(2)} \geq R_{\min}^c, \forall i; \end{aligned} \quad (29)$$

Similar to \mathbf{P}_1 , \mathbf{P}_4 is extremely difficult to solve due to the fractional objective function and multiple coupled variables. Next, we transform \mathbf{P}_4 into a more tractable form.

B. PROBLEM TRANSFORMATION

Since the numerator of the objective function of \mathbf{P}_4 , i.e., R_{sum}^{CSR} in (15), is a monotonically increasing function of z_i , the system EE is maximized when the harvested energy of each BD equals their circuit power consumption, that is

$$t_i P_i h_i^{t,b} (1 - z_i) \eta = t_i P_{cir}^{BD}, \quad (30)$$

and the optimal reflection coefficient z_i^* is obtained as

$$z_i^* = 1 - \frac{P_{cir}^{BD}}{P_i h_i^{t,b} \eta}. \quad (31)$$

Remark 2: According to (31), the optimal reflection coefficient in the CSR case increases with higher PT transmission power, which is opposite to the PSR case. This is because in CSR, the backscatter links not only cause no interference to the primary link, but also enhance the throughput of the primary link.

Based on (31) and letting $B_i = \frac{P_{cir}^{BD} h_i^{r,b}}{\eta}$, \mathbf{P}_4 is transformed into

$$\begin{aligned} P_5 : \max_{\{P_i, t_i\}} & W \frac{\sum_{i=1}^M t_i \left[\log_2 \left(\frac{P_i h^{t,r}}{\sigma^2} \right) - \text{Ei} \left(-\frac{h^{t,r}}{A_i - \frac{B_i}{P_i}} \right) \log_2 e \right] + \sum_{i=1}^M t_i \frac{1}{N} \log_2 \left(1 + \frac{N(P_i A_i - B_i)}{\sigma^2} \right)}{\sum_{i=1}^M t_i (P_i + P_{cir}^{TR})} \\ \text{s.t.} & C1, C3, C4 - 3; \\ & C2 - 2 : 0 \leq 1 - \frac{P_{cir}^{BD}}{P_i h_i^{t,b} \eta} \leq 1, \forall i. \end{aligned} \quad (32)$$

Then, by introducing the auxiliary variables $U_i = (P_i A_i - B_i) t_i$, $i \in \mathcal{M}$, substituting $P_i = B_i / A_i + U_i / (t_i A_i)$ into (32) and employing the Dinkelbach-based method on the objective function of \mathbf{P}_5 , we transform \mathbf{P}_5 into

$$P_6 : \max_{\{t_i, U_i\}} W \sum_{i=1}^M t_i \left[\log_2 \left(\frac{(B_i + \frac{U_i}{t_i}) h^{t,r}}{A_i \sigma^2} \right) \right]$$

$$\begin{aligned}
 & - \text{Ei} \left(- \frac{h^{t,r}}{A_i - \frac{A_i B_i}{(B_i + \frac{U_i}{t_i})}} \right) \log_2 e \Big] \\
 & + W \sum_{i=1}^M t_i \frac{1}{N} \log_2 \left(1 + \frac{N U_i}{t_i \sigma^2} \right) \\
 & - Q \sum_{i=1}^M t_i \left(\frac{B_i + \frac{U_i}{t_i}}{A_i} + P_{cir}^{TR} \right) \\
 \text{s.t. C3;} \\
 \text{C1 - 1 : } & 0 \leq \frac{B_i + \frac{U_i}{t_i}}{A_i} \leq P_{\max}, \forall i; \\
 \text{C2 - 3 : } & 0 \leq 1 - \frac{P_{cir}^{BD} A_i}{\left(B_i + \frac{U_i}{t_i} \right) h_i^{t,b} \eta} \leq 1, \forall i; \\
 \text{C4 - 4 : } & R^{s(2)'} \geq R_{\min}^s, R_i^{c(2)'} \geq R_{\min}^c, \forall i, \quad (33)
 \end{aligned}$$

where

$$R^{s(2)'} = W \sum_{i=1}^M t_i \begin{bmatrix} \log_2 \left(\frac{(B_i + \frac{U_i}{t_i}) h^{t,r}}{A_i \sigma^2} \right) \\ - \text{Ei} \left(- \frac{h^{t,r}}{A_i - \frac{A_i B_i}{(B_i + \frac{U_i}{t_i})}} \right) \log_2 e \end{bmatrix}$$

$$\text{and } R_i^{c(2)'} = W \sum_{i=1}^M t_i \frac{1}{N} \log_2 \left(1 + \frac{N U_i}{t_i \sigma^2} \right).$$

C. PROBLEM SOLUTION

To solve \mathbf{P}_6 , we apply the SCP technique on $R^{s(2)'}$ to transform it into a convex form and successively maximize the lower bound of the objective function in an iterative manner based on the following lemma.

Lemma 4: For any given $P_i^{(j)} = B_i^{(j)} / A_i + U_i^{(j)} / (t_i^{(j)} A_i)$, $j > 0$, where $P_i^{(j)}$, $B_i^{(j)}$, $U_i^{(j)}$ and $t_i^{(j)}$ denote the obtained parameter values after the j th iteration, we have

$$R^{s(2)}(P_i) \geq R^{s(2)}(P_i^{(j)}), \forall i, \quad (34)$$

where

$$\begin{aligned}
 & R^{s(2)}(P_i^{(j)}) \\
 & = W \sum_{i=1}^M t_i \left[\log_2 \left(\frac{P_i^{(j)} h^{t,r}}{\sigma^2} \right) - \text{Ei} \left(- \frac{h^{t,r}}{A_i - \frac{B_i}{P_i^{(j)}}} \right) \right. \\
 & \quad \left. \log_2 e + \left(\frac{\log_2 e}{P_i^{(j)}} + \frac{B_i \exp \left(- \frac{h^{t,r}}{A_i - \frac{B_i}{P_i^{(j)}}} \right) \log_2 e}{A_i (P_i^{(j)})^2 - B_i P_i^{(j)}} \right) \right. \\
 & \quad \left. (P_i - P_i^{(j)}) \right], \quad (35)
 \end{aligned}$$

and the equalities in (34) only hold when $P_i = P_i^{(j)}$.

Proof: Please see Appendix C. ■

By substituting (35) into (33) and after some manipulations, $\mathbf{P}_{6.1}$ is equivalently formulated as

$$\begin{aligned}
 \mathbf{P}_{6.1} : \{U_i^*, t_i^*\} = F_3 = \arg \max_{\{U_i, t_i\}} & W \sum_{i=1}^M t_i \\
 & \times \left[\log_2 \left(\frac{P_i^{(j)} h^{t,r}}{\sigma^2} \right) - \text{Ei} \left(- \frac{h^{t,r}}{A_i - \frac{B_i}{P_i^{(j)}}} \right) \log_2 e \right. \\
 & \quad \left. + \left(\frac{\log_2 e}{P_i^{(j)}} + \frac{B_i \exp \left(- \frac{h^{t,r}}{A_i - \frac{B_i}{P_i^{(j)}}} \right) \log_2 e}{A_i P_i^{(j)} - B_i P_i^{(j)}} \right) \left(\frac{B_i}{A_i} - P_i^{(j)} \right) \right] \\
 & + W \sum_{i=1}^M \frac{U_i}{A_i} \left(\frac{\log_2 e}{P_i^{(j)}} + \frac{B_i \exp \left(- \frac{h^{t,r}}{A_i - \frac{B_i}{P_i^{(j)}}} \right) \log_2 e}{A_i P_i^{(j)} - B_i P_i^{(j)}} \right) \\
 & + W \sum_{i=1}^M t_i \frac{1}{N} \log_2 \left(1 + \frac{N U_i}{t_i \sigma^2} \right) - Q \sum_{i=1}^M \left(\frac{B_i t_i + U_i}{A_i} + P_{cir}^{TR} \right) \\
 \text{s.t. C3; C4 - 4;} \\
 \text{C1 - 2 : } & U_i \leq t_i (P_{\max} A_i - B_i), \forall i; \\
 \text{C2 - 4 : } & U_i \geq 0, \forall i. \quad (36)
 \end{aligned}$$

It is observed that the first term and the third term of the objective function in (36) are linear with respect to U_i and t_i , and the second term of the objective function is a standard log-form convex function. Therefore, $\mathbf{P}_{6.1}$ is jointly convex with respect to U_i and t_i , and can be solved using the interior point method.

Lemma 5: To gain more insights, we derive the closed form expression of the optimal PT transmission power P_i by employing the Lagrange dual method as follows.

$$\begin{aligned}
 P_i^* & = \frac{B_i}{A_i} + \frac{1}{N A_i} \\
 & \times \left[\frac{A_i (1 + \delta_i) \log_2 e}{Y - (1 + \beta) \left(\frac{\log_2 e}{P_i^{(j)}} + \frac{B_i \exp \left(- \frac{h^{t,r}}{A_i - \frac{B_i}{P_i^{(j)}}} \right) \log_2 e}{A_i P_i^{(j)} - B_i P_i^{(j)}} \right)} - \sigma^2 \right], \quad (37)
 \end{aligned}$$

Algorithm 1 Dinkelbach Based Iterative Algorithm

Input: \mathcal{M} .

Output: $Q^*, t_i^*, L_i^*, P_i^*, U_i^*$.

Initialize: $j = 1, v = 1, Q(v), \epsilon$.

- 1: In the case of PSR
 - 2: **repeat**
 - 3: **repeat**
 - 4: Initialize $L_i^{(j)}, t_i^{(j)}$;
 - 5: **repeat**
 - 6: Obtain t_i, L_i by solving $\mathbf{P}_{3.1}$;
 - 7: $j = j + 1$;
 - 8: **until** the objective function value in $\mathbf{P}_{3.1}$ converges;
 - 9: Obtain P_i by solving $\mathbf{P}_{3.2}$;
 - 10: **until** the objective function value in \mathbf{P}_3 converges;
 - 11: Compute $R_i^{s(1)'}$ and $R_i^{c(1)'}$ in (20);
 - 12: $v = v + 1$;
 - 13: Update $Q(v) = \frac{R_i^{s(1)'} + \sum_{i=1}^M R_i^{c(1)'}}{\sum_{i=1}^M t_i(P_i + P_{cir}^{BD})}$;
 - 14: **until** $|\min_{i \in \mathcal{M}} R_i^{s(1)'} + \sum_{i=1}^M R_i^{c(1)'} - Q(v) \sum_{i=1}^M t_i(P_i + P_{cir}^{BD})| \leq \epsilon$.
 - 15: In the case of CSR
 - 16: **repeat**
 - 17: Initialize $U_i^{(j)}, t_i^{(j)}$;
 - 18: **repeat**
 - 19: Obtain U_i, t_i by solving $\mathbf{P}_{6.1}$;
 - 20: $j = j + 1$;
 - 21: **until** the objective function value in $\mathbf{P}_{6.1}$ converges;
 - 22: Compute $R_i^{s(2)'}$ and $R_i^{c(2)'}$ in (33);
 - 23: $v = v + 1$;
 - 24: Update $Q(v) = \frac{R_i^{s(2)'} + \sum_{i=1}^M R_i^{c(2)'}}{\sum_{i=1}^M t_i(P_i + P_{cir}^{BD})}$;
 - 25: **until** $|\min_{i \in \mathcal{M}} R_i^{s(2)'} + \sum_{i=1}^M R_i^{c(2)'} - Q(v) \sum_{i=1}^M t_i(P_i + P_{cir}^{BD})| \leq \epsilon$.
-

where $Y = Q + A_i \varepsilon_i$, and $\beta, \delta_i, \varepsilon_i$ are the Lagrange multipliers associated with C4-4 and C1-2, respectively.

Proof: Please see Appendix D. ■

Remark 3: According to (37), the optimal PT transmission power increases with a higher channel power gain of the primary link, i.e., $h^{t,r}$, leading to a higher system EE.

V. DINKELBACH BASED ITERATIVE ALGORITHM

Based on the solutions obtained in Sections III and IV, we propose a Dinkelbach-based iterative algorithm in **Algorithm 1** to solve \mathbf{P}_3 and \mathbf{P}_6 for the PSR and CSR cases, respectively, where v is the iteration index for updating the maximum system EE Q^* , and ϵ is the convergence threshold imposed on the objective function in \mathbf{P}_3 and \mathbf{P}_6 , by meeting which the algorithm terminates.

VI. CONVERGENCE AND COMPUTATIONAL COMPLEXITY ANALYSIS

We first analyze the convergence of **Algorithm 1**. The SCP based iterative method applied for solving $\mathbf{P}_{3.1}$ and $\mathbf{P}_{6.1}$ ensures that the objective function value of them monotonically increases with the iteration, because the objective functions in $\mathbf{P}_{3.1}$ and $\mathbf{P}_{6.1}$ are the lower bound functions of those in \mathbf{P}_3 and \mathbf{P}_6 , respectively. Meanwhile, $\mathbf{P}_{3.1}$ and $\mathbf{P}_{6.1}$ are upper bounded by their constraints. Thus, the SCP based iterative method is guaranteed to converge to a locally optimal solution. The BCD method used to solve \mathbf{P}_3 also ensures that the solution converges to a locally optimal value, because the objective function value of \mathbf{P}_3 is nondecreasing with updated variables after each iteration, and it is also upper bounded by its associated constraints.

Then, we evaluate the computational complexity of **Algorithm 1**. For the PSR case, the computational complexity of the interior point method used to solve $\mathbf{P}_{3.1}$ and $\mathbf{P}_{3.2}$ is $\mathcal{O}(\sqrt{N_1} \frac{1}{\zeta_1})$ and $\mathcal{O}(\sqrt{N_2} \frac{1}{\zeta_2})$, respectively, where $N_1 = 2M$, $N_2 = M$ denote the number of variables, and ζ_1, ζ_2 represent the iterative accuracy [31], [32]. Denoting the number of iterations required for the convergence of the SCP method, the BCD method and the maximum EE Q^* by Δ_1, Δ_2 and Δ_3 , respectively, the total computational complexity of **Algorithm 1** for the PSR case is $\mathcal{O}[\Delta_2 \Delta_3 (\Delta_1 \sqrt{N_1} \frac{1}{\zeta_1} + \sqrt{N_2} \frac{1}{\zeta_2})]$. For the CSR case, the computational complexity of the interior point method used to solve $\mathbf{P}_{6.1}$ is $\mathcal{O}(\sqrt{N_3} \frac{1}{\zeta_3})$, where $N_3 = 2M$ is the number of variables and ζ_3 represents the iterative accuracy. Denoting the number of iterations required for the convergence of the SCP method and the maximum EE Q^* by Δ_4 and Δ_5 , respectively, the total computational complexity of **Algorithm 1** for the CSR case is $\mathcal{O}(\Delta_4 \Delta_5 \sqrt{N_3} \frac{1}{\zeta_3})$ [31], [32].

VII. SIMULATION RESULTS

In this section, we present the simulation results to evaluate the system EE performance versus the system parameters, e.g., the PT-PR distance, and the throughput requirements for the backscatter link and the primary link. The convergence of **Algorithm 1** and the throughput performance are also evaluated. The simulation parameters are set as follows unless otherwise specified. The number of the BDs $M = 5, N = 100$ for the CSR case, the PT-PR distance $r = 20$ m, the pathloss exponent $\alpha = 3$, the channel bandwidth $W = 10$ kHz, the AWGN power spectral density is -130 dBm/Hz, the maximum PT transmission power $P_{max} = 23$ dBm, the energy conversion efficiency $\eta = 0.6$, the backscatter circuit power consumption $P_{cir}^{BD} = 200$ μ W, the PT and PR's total circuit power consumption $P_{cir}^{TR} = 2$ mW, and the convergence threshold $\epsilon = 10^{-10}$. We assume that the minimum throughput requirement for each backscatter link is the same.

A. CONVERGENCE OF ALGORITHM 1

Fig. 2 shows the convergence of **Algorithm 1**. We can see that the system EE in both the PSR and CSR cases converges quickly after the 3rd iteration. The system EE in the PSR case

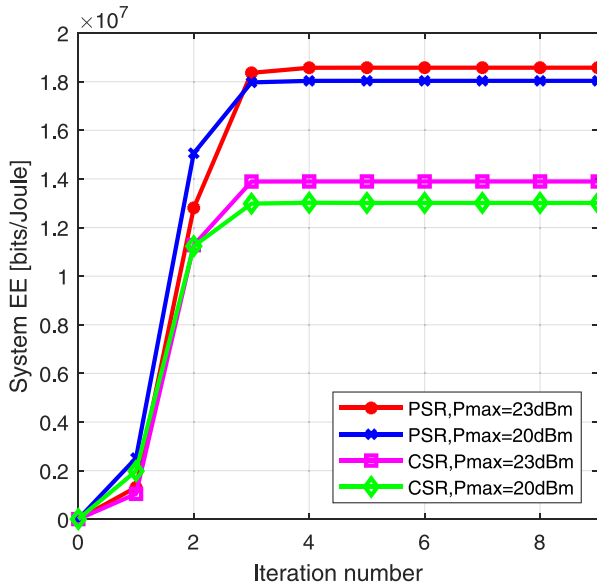


FIGURE 2. Convergence of Algorithm 1.

is higher than that in the CSR case. This is because due to the long BD symbol period, the throughput of the backscatter link in the CSR case is lower than that in the PSR case, thus the system EE is reduced. Moreover, the throughput of the primary link in the CSR case is higher than that in the PSR case, but the system EE improvement brought by the higher throughput cannot compensate for the EE loss due to the higher PT transmission power for meeting R_{min}^c . Therefore, the system EE decreases with higher power consumption. In addition, the system EE increases with higher maximum PT transmission power in both the PSR and CSR cases. This is because the optimal PT transmission power for maximizing the system EE is capped at P_{max} and a higher P_{max} leads to a higher system EE.

B. SYSTEM EE PERFORMANCE

Fig. 3 plots the system EE versus the PT-PR distance r for different values of N . It can be seen that the system EE in both the PSR and CSR cases reduce with a longer r . The reason is that the longer r decreases the received power at the PR, which reduces the throughput of the primary link and the system EE. In addition, the system EE in the CSR case is higher with a lower N . This is because the backscatter link can achieve a higher throughput with a shorter BD symbol period. When the value of N reaches 200, the system EE of the CSR case reduces to 0 when r is longer than 15m. This is because the throughput requirements of the BDs in the CSR case cannot be satisfied due to the very long symbol period of the BackCom for $N = 200$.

Fig. 4(a) illustrates the system EE versus R_{min}^c in the PSR case under different R_{min}^s . We can see that the system EE decreases with a higher R_{min}^c . This is because a higher backscatter link throughput requirement needs the PT to increase its transmission power, while the EE improvement

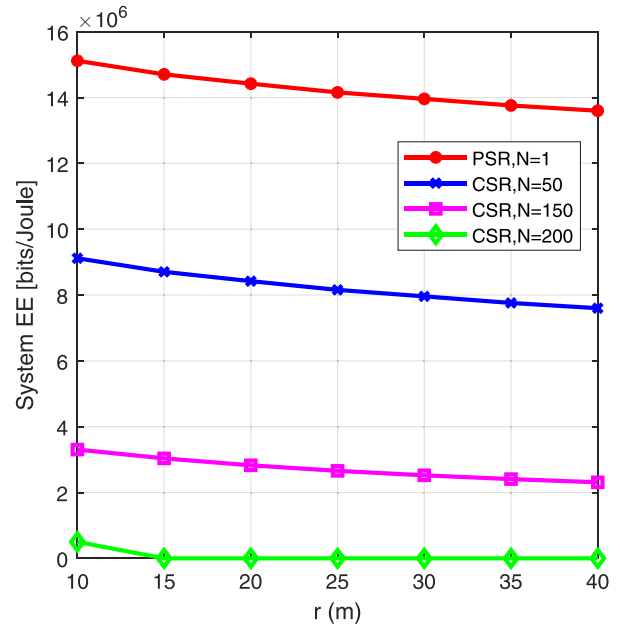


FIGURE 3. System EE versus PT-PR distance r .

due to a higher backscatter link throughput cannot compensate for the EE loss due to more energy consumption. However, the system EE keeps the same when R_{min}^s increases from 3M bits/s to 4M bits/s. This indicates that the primary link throughput obtained under the optimal solution for maximizing the system EE is higher than 4M bits/s. When R_{min}^s increases beyond 4.7M bits/s, the PT needs to increase its transmission power, which results in system EE reduction.

Fig. 4(b) demonstrates the system EE versus R_{min}^c in the CSR case under different R_{min}^s . We can see that the system EE decreases with R_{min}^c in the CSR case much faster than that in the PSR case. This is because due to long BD symbol period in CSR, higher PT transmission power is required to meet R_{min}^c , which greatly reduces the system EE. When R_{min}^c exceeds 17k bits/s, even the maximum PT transmission power cannot let the BDs meet the throughput requirement, thus the system EE drops to 0.

By comparing Fig. 4(a) with Fig. 4(b), we find that the system EE in the CSR case exceeds that in the PSR case when R_{min}^c is between 3k bits/s and 13k bits/s and R_{min}^s is larger than 47k bits/s. Since the BD signal is regarded as an interference signal in the PSR case while being treated as a multipath component in the CSR case, the PT needs to transmit at a higher power level to meet the primary link throughput requirement in PSR than in CSR, which reduces the system EE in the PSR case.

C. THROUGHPUT PERFORMANCE

Fig. 5(a) shows the throughput of each Backscatter link under different R_{min}^s and R_{min}^c in the PSR. It is clear to see that each backscatter link maintains the minimum required throughput R_{min}^c even when R_{min}^s is changed. This proves that the primary link dominates the system EE and the maximum system EE

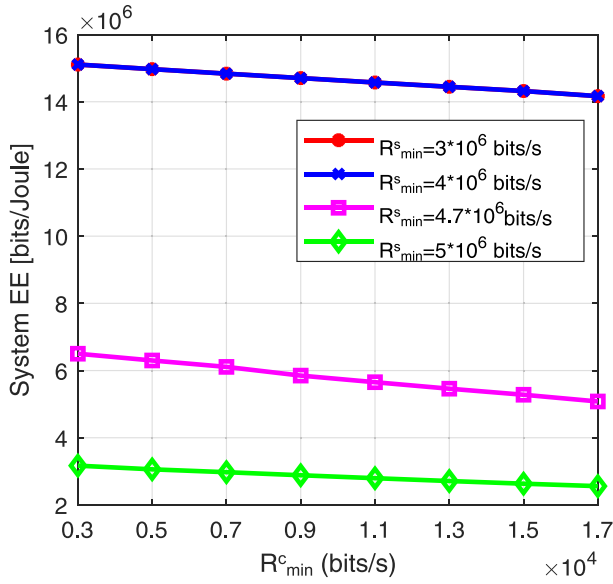
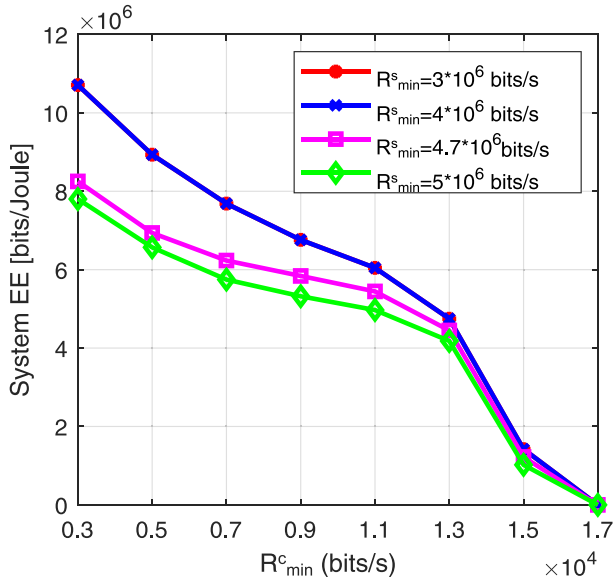
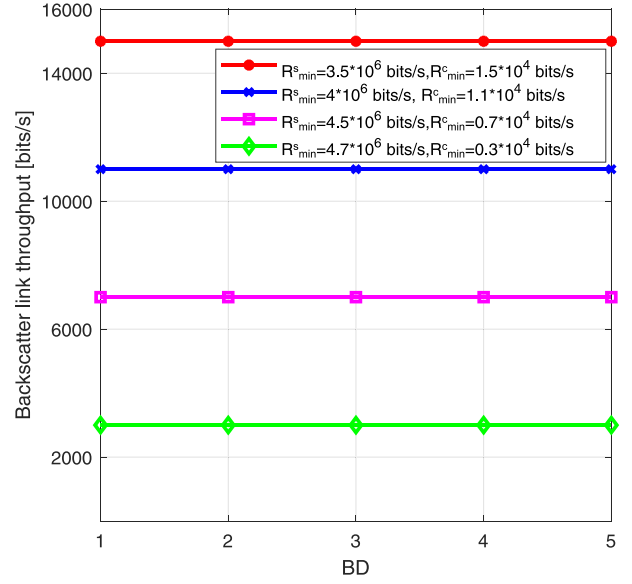

 (a). System EE versus R_{min}^c (PSR)

 (b). System EE versus R_{min}^c (CSR)

FIGURE 4. (a) System EE versus R_{min}^c (PSR). (b) System EE versus R_{min}^c (CSR).

is achieved when each BD adjusts its reflection coefficient to minimize its interference to the primary link while meeting its own throughput requirement R_{min}^c .

Fig. 5(b) plots the primary link throughput versus R_{min}^c under different R_{min}^s in the PSR case. For R_{min}^s being 3M bits/s and 4M bits/s, the primary link throughput is the same and it reduces with a higher R_{min}^c . This is because a higher R_{min}^c needs a higher reflection coefficient, but then the interference power from each BD also becomes larger and the primary link throughput reduces. In addition, when R_{min}^s is higher than 4.7M bits/s, the maximum system EE is achieved when the PT transmission power is just sufficient



(a). Backscatter link throughput for different BD (PSR)

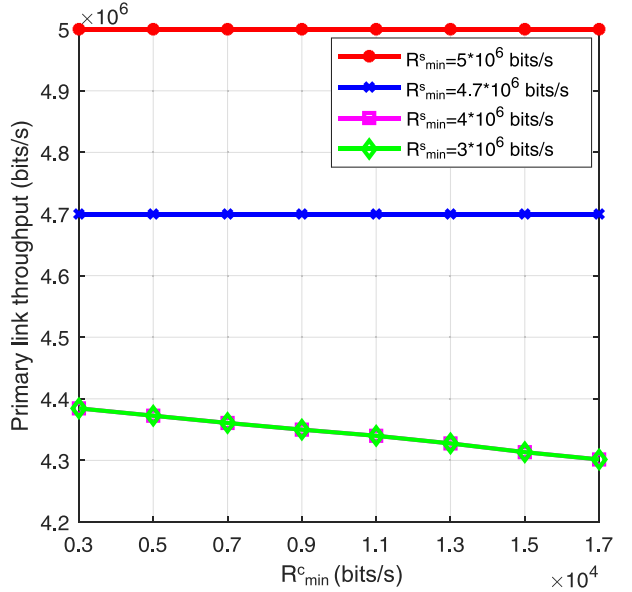
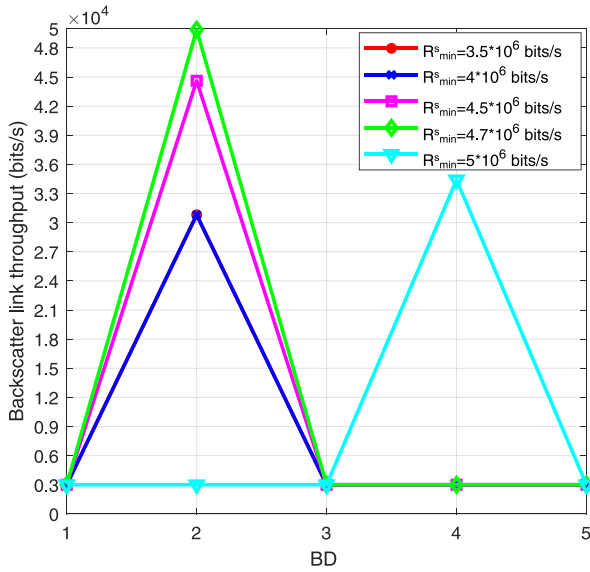

 (b). Primary link throughput versus R_{min}^c (PSR)

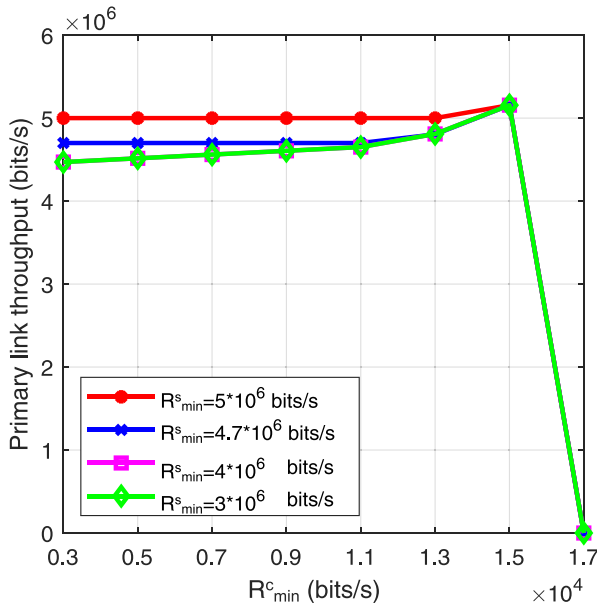
FIGURE 5. (a) Backscatter link throughput for different BD (PSR). (b) Primary link throughput versus R_{min}^c (PSR).

to meet R_{min}^s which would be sufficient to meet all the considered values of R_{min}^c as well. Thus, increasing R_{min}^c does not affect the primary link throughput, while any increase of the PT transmission power beyond the sufficient level will decrease the system EE.

Fig. 6(a) illustrates the throughput of each Backscatter link under different R_{min}^s for $R_{min}^c = 3$ k bits/s in the CSR case. We find that for each considered value of R_{min}^s , only one BD achieves a throughput higher than R_{min}^c . This is because that this BD has the potential to contribute more to the system EE than the other BDs, thus is allocated the maximum allowed



(a). Backscatter link throughput for different BD (CSR)



(b). Primary link throughput versus R_{min}^c (CSR)

FIGURE 6. (a) Backscatter link throughput for different BD (CSR). (b) Primary link throughput versus R_{min}^c (CSR).

time for backscattering, while the remained time is allocated to the other BDs for meeting R_{min}^c . Moreover, the BD that is allocated the maximum allowed time for backscattering may change with different R_{min}^s . This is because different values of R_{min}^s may require different PT transmission power, which affects the backscatter link throughput achievable by each BD.

Fig. 6(b) demonstrates the primary link throughput versus R_{min}^c under different R_{min}^s in the CSR case. When R_{min}^s is lower than 4M bits/s and R_{min}^c is no larger than 15k bit/s, the primary link throughput increases with R_{min}^c . This is because

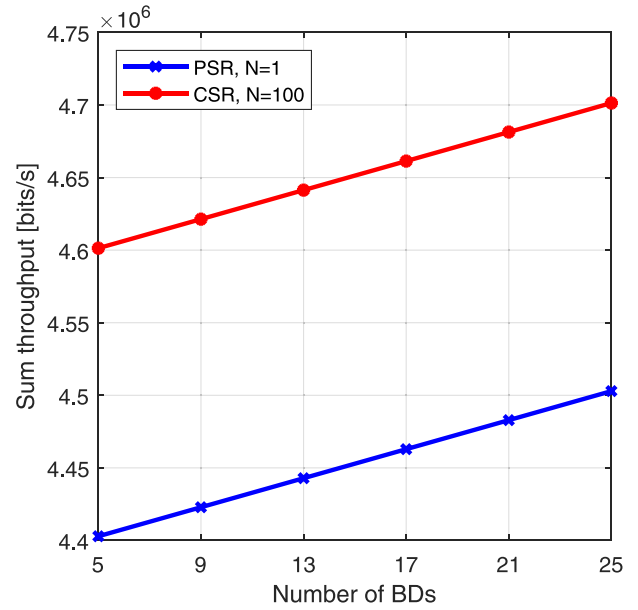


FIGURE 7. Sum throughput versus the number of BDs ($R_{min}^c = 5kbits/s$).

the PT transmission power for meeting low values of R_{min}^s is not sufficient to meet R_{min}^c and the PT transmission power has to increase for a higher R_{min}^c , thus resulting in a higher primary link throughput. When R_{min}^s exceeds 4.7M bits/s, the primary link throughput first keeps constant and then increases with R_{min}^c . This is because the PT transmission power for meeting large values of R_{min}^s can satisfy relatively small values of R_{min}^c but will have to increase for meeting larger values of R_{min}^c . When R_{min}^c reaches 17k bit/s, each BD has to use a very large reflection coefficient to meet this high throughput requirement, causing excessive interference to the primary link, while the PT transmission power being capped at P_{max} , hence the primary link throughput drops to 0.

Fig. 7 demonstrates that the sum throughput of the primary link and the backscatter links increases linearly with the number of BDs in both the PSR and CSR cases. This is because in the PSR case, the increase of the sum throughput is mainly brought by the more backscatter links, each maintaining the minimum throughput requirement, i.e., R_{min}^c ; while similarly in the CSR case, apart from one BD achieving a throughput higher than R_{min}^c , all the other BDs also maintain the minimum throughput requirement, hence the sum throughput increases linearly with more BDs. For each considered number of BDs, the sum throughput of the CSR case is higher than that of the PSR case. This is because in the CSR case, one BD can achieve a throughput much higher than R_{min}^c , while the backscatter links helping improve the throughput of the primary link.

VIII. CONCLUSION

In this paper, we have investigated the system EE maximization problem in an SR system, where multiple BDs share the same RF channel with a primary link, for both

the PSR and CSR cases. Since the formulated system EE maximization problem is extremely difficult to solve directly, we propose a Dinkelbach-based iterative algorithm to first transform the optimization problem into a more tractable form by introducing auxiliary variables and using the generalized fractional programming, then employ the BCD method and the SCP technique to solve the transformed problem in an iterative manner. The simulation results demonstrate that the proposed algorithm converges very fast and the maximized system EE reduces with a longer PT-PR distance and a higher throughput requirement per link. Moreover, we find that the primary link dominates the system EE and the maximum system EE is achieved when the BD that has the potential to obtain the highest throughput among all BDs (which depends on the PT transmission power in the corresponding time slot) is allocated the maximum allowed time for backscattering, while guaranteeing the throughput requirement of the other BDs.

APPENDIX A PROOF OF LEMMA 2

Let us define a function given by $f_1 = \log_2\left(1 + \frac{P_i h^{t,r}}{A_i X_i^{(j)} + \sigma^2}\right)$, where f_1 is convex with respect to X_i . Since the first-order Taylor expansion of a convex function is a global under-estimator of its function values. For any given $X_i^{(j)}$, we have

$$f_1 \geq \log_2\left(1 + \frac{P_i h^{t,r}}{A_i X_i^{(j)} + \sigma^2}\right) - \frac{P_i h^{t,r} A_i \log_2 e}{(A_i X_i^{(j)} + \sigma^2 + P_i h^{t,r})(A_i X_i^{(j)} + \sigma^2)} \left(\frac{L_i}{t_i} - X_i^{(j)}\right), \quad (38)$$

where the equalities hold when $\frac{L_i}{t_i} = X_i^{(j)}$. The proof is completed.

APPENDIX B PROOF OF LEMMA 3

Based on the Lagrange dual method, $\mathbf{P}_{3.1}$ is equivalently transformed into

$$\begin{aligned} \mathbb{L}_1 = & \min_{\beta, \delta_i, \lambda, \mu_i, \varepsilon_i} \max_{L_i, t_i} F_1 \\ & + \beta W \left[t_i \log_2 \left(1 + \frac{P_i h^{t,r}}{A_i X_i^{(j)} + \sigma^2} \right) - \frac{P_i h^{t,r} A_i \log_2 e}{(A_i X_i^{(j)} + \sigma^2 + P_i h^{t,r})(A_i X_i^{(j)} + \sigma^2)} \right. \\ & \quad \left. \times (L_i - t_i X_i^{(j)}) - R_{\min}^s \right] \\ & + \sum_{i=1}^M \delta_i W \left[\mathbb{E}_s \left[t_i \log_2 \left(1 + \frac{A_i L_i |s(n)|^2}{t_i \sigma^2} \right) \right] - R_{\min}^c \right] \\ & + \lambda \left(T - \sum_{i=1}^M t_i \right) + \sum_{i=1}^M \mu_i (P_i t_i - L_i) \end{aligned}$$

$$+ \sum_{i=1}^M \varepsilon_i \left[t_i \left(P_i - \frac{P^{BD}_{cir}}{h_i^{t,b} \eta} \right) - L_i \right]. \quad (39)$$

Since $\mathbf{P}_{3.1}$ is convex, (39) is convex. Applying the KKT conditions and letting $\frac{\partial \mathbb{L}_1}{\partial L_i} = 0$, we obtain

$$X_i = \frac{L_i}{t_i} = \frac{(1 + \delta_i) \log_2 e}{\mu_i + \varepsilon_i + (1 + \beta) \frac{P_i h^{t,r} A_i \log_2 e}{(A_i X_i^{(j)} + \sigma^2 + P_i h^{t,r})(A_i X_i^{(j)} + \sigma^2)}} - \frac{\sigma^2}{A_i \mathbb{E}_s |s(n)|^2}. \quad (40)$$

By substituting (40) into $Z_i = \frac{X_i}{P_i}$, Z_i^* is obtained. $\mathbf{P}_{3.2}$ can also be transformed into

$$\begin{aligned} \mathbb{L}_2 = & \min_{\beta, \mu_i, \varepsilon_i} \max_{P_i} F_2 \\ & + \beta W \left[\sum_{i=1}^M t_i \log_2 \left(1 + \frac{P_i h^{t,r}}{A_i X_i + \sigma^2} \right) - R_{\min}^s \right] \\ & + \sum_{i=1}^M \mu_i (P_{\max} - P_i) + \sum_{i=1}^M \varepsilon_i \left(P_i - X_i - \frac{P^{BD}_{cir}}{h_i^{t,b} \eta} \right). \end{aligned} \quad (41)$$

Since $\mathbf{P}_{3.2}$ is convex, (41) is convex. Applying the KKT conditions and letting $\frac{\partial \mathbb{L}_2}{\partial P_i} = 0$, we obtain

$$P_i^* = \frac{(1 + \beta) \log_2 e}{Q + \frac{\mu_i - \varepsilon_i}{t_i}} - \frac{A_i X_i + \sigma^2}{h^{t,r}}. \quad (42)$$

The optimal values of z_i and P_i are obtained and the proof is completed.

APPENDIX C PROOF OF LEMMA 4

Let us define a function $f_2 = \log_2\left(\frac{P_i h^{t,r}}{\sigma^2}\right) - \text{Ei}\left(-\frac{h^{t,r}}{A_i - \frac{P^{BD}_{cir} h_i^{r,b}}{P_i \eta}}\right) \log_2 e$, where f_2 is convex with respect to P_i . Since the first-order Taylor expansion of a convex function is a global under-estimator of its function values. For any given $P_i^{(j)}$, we have

$$\begin{aligned} f_2 \geq & \log_2 \left(\frac{P_i^{(j)} h^{t,r}}{\sigma^2} \right) - \text{Ei} \left(- \frac{h^{t,r}}{A_i - \frac{P^{BD}_{cir} h_i^{r,b}}{P_i^{(j)} \eta}} \right) \log_2 e \\ & + \left(\frac{\log_2 e}{P_i^{(j)}} + \frac{B_i e^{-\frac{h^{t,r}}{A_i - \frac{B_i}{P_i^{(j)}}}} \log_2 e}{A_i P_i^{(j)} - B_i P_i^{(j)}} \right) (P_i - P_i^{(j)}), \end{aligned} \quad (43)$$

where the equalities hold when $P_i = P_i^{(j)}$. The proof is completed.

APPENDIX D PROOF OF LEMMA 5

Based on the Lagrange dual method, $\mathbf{P}_{6.1}$ is equivalently transformed into

$$\begin{aligned} \mathbb{L}_3 = & \min_{\beta, \delta_i, \lambda, \varepsilon_i} \max_{U_i, t_i} F_3 \\ & + \beta \left(W \sum_{i=1}^M t_i \left[\log_2 \left(\frac{P_i^{(j)} h^{t,r}}{\sigma^2} \right) - \text{Ei} \left(- \frac{h^{t,r}}{A_i - \frac{P_i^{BD} h_i^{t,b}}{P_i^{(j)} \eta}} \right) \log_2 e \right. \right. \\ & \quad \left. \left. + \left(\frac{\log_2^e}{P_i^{(j)}} + \frac{B_i e^{-\frac{h^{tr}}{A_i - \frac{B_i}{P_i^{(j)}}}} \log_2^e}{A_i P_i^{(j)} - B_i P_i^{(j)}} \right) \right. \right. \\ & \quad \left. \left. \left(\frac{B_i}{A_i} - P_i^{(j)} \right) \right] \right. \\ & \quad \left. + W \sum_{i=1}^M \frac{U_i}{A_i} \left(\frac{\log_2^e}{P_i^{(j)}} + \frac{B_i e^{-\frac{h^{tr}}{A_i - \frac{B_i}{P_i^{(j)}}}} \log_2^e}{A_i P_i^{(j)} - B_i P_i^{(j)}} \right) - R_{\min}^s \right) \\ & + \sum_{i=1}^M \delta_i W \left[\sum_{i=1}^M t_i \frac{1}{N} \log_2 \left(1 + \frac{N U_i}{t_i \sigma^2} \right) - R_{\min}^c \right] \\ & + \lambda \left(T - \sum_{i=1}^M t_i \right) + \sum_{i=1}^M \varepsilon_i [t_i (P_{\max} A_i - B_i) - U_i]. \quad (44) \end{aligned}$$

Since $\mathbf{P}_{6.1}$ is convex, (44) is convex. Applying the KKT conditions and letting $\frac{\partial \mathbb{L}_3}{\partial U_i} = 0$, we obtain

$$\frac{U_i}{t_i} = \frac{1}{N} \left[\frac{(1 + \delta_i) \log_2 e}{(1 + \beta) \left(\frac{\log_2^e}{P_i^{(j)}} + \frac{B_i e^{-\frac{h^{tr}}{A_i - \frac{B_i}{P_i^{(j)}}}} \log_2^e}{A_i P_i^{(j)} - B_i P_i^{(j)}} \right)} - \sigma^2 \right]. \quad (45)$$

Substituting (45) into $P_i = \frac{B_i + U_i}{A_i}$, the optimal value of P_i is obtained and the proof is completed.

REFERENCES

- [1] L. Chettri and R. Bera, "A comprehensive survey on Internet of Things (IoT) toward 5G wireless systems," *IEEE Internet Things J.*, vol. 7, no. 1, pp. 16–32, Jan. 2020.
- [2] R. Long, Y.-C. Liang, H. Guo, G. Yang, and R. Zhang, "Symbiotic radio: A new communication paradigm for passive Internet of Things," *IEEE Internet Things J.*, vol. 7, no. 2, pp. 1350–1363, Feb. 2020.
- [3] Y.-C. Liang, K.-C. Chen, G. Y. Li, and P. Mahonen, "Cognitive radio networking and communications: An overview," *IEEE Trans. Veh. Technol.*, vol. 60, no. 7, pp. 3386–3407, Sep. 2011.
- [4] A. A. Khan, M. H. Rehmani, and A. Rachedi, "Cognitive-radio-based Internet of Things: Applications, architectures, spectrum related functionalities, and future research directions," *IEEE Wireless Commun.*, vol. 24, no. 3, pp. 17–25, Jun. 2017.
- [5] L. Zhang, Y.-C. Liang, and M. Xiao, "Spectrum sharing for Internet of Things: A survey," *IEEE Wireless Commun.*, vol. 26, no. 3, pp. 132–139, Jun. 2019.
- [6] Y. C. Liang, Q. Zhang, E. G. Larsson, and G. Y. Li, "Symbiotic radio: Cognitive backscattering communications for future wireless networks," *IEEE Trans. Cogn. Commun. Netw.*, vol. 6, no. 4, pp. 1242–1255, Dec. 2020.
- [7] X. Kang, Y.-C. Liang, and J. Yang, "Riding on the primary: A new spectrum sharing paradigm for wireless-powered IoT devices," *IEEE Trans. Wireless Commun.*, vol. 17, no. 9, pp. 6335–6347, Sep. 2018.
- [8] G. Yang, D. Yuan, Y.-C. Liang, R. Zhang, and V. C. M. Leung, "Optimal resource allocation in full-duplex ambient backscatter communication networks for wireless-powered IoT," *IEEE Internet Things J.*, vol. 6, no. 2, pp. 2612–2625, Apr. 2019.
- [9] Y. Zhang, B. Li, F. Gao, and Z. Han, "A robust design for ultra reliable ambient backscatter communication systems," *IEEE Internet Things J.*, vol. 6, no. 5, pp. 8989–8999, Oct. 2019.
- [10] D. Li, "Two birds with one stone: Exploiting decode-and-forward relaying for opportunistic ambient backscattering," *IEEE Trans. Commun.*, vol. 68, no. 3, pp. 1405–1416, Mar. 2020.
- [11] C. Boyer and S. Roy, "Invited Paper: Backscatter communication and RFID: Coding, energy, and MIMO analysis," *IEEE Trans. Commun.*, vol. 62, no. 3, pp. 770–785, Mar. 2014.
- [12] B. Ji, Z. Chen, S. Chen, B. Zhou, C. Li, and H. Wen, "Joint optimization for ambient backscatter communication system with energy harvesting for IoT," *Mech. Syst. Signal Process.*, vol. 135, Jan. 2020, Art. no. 106412.
- [13] H. Yang, Y. Ye, and X. Chu, "Max-min energy-efficient resource allocation for wireless powered backscatter networks," *IEEE Wireless Commun. Lett.*, vol. 9, no. 5, pp. 688–692, May 2020.
- [14] N. Van Huynh, D. T. Hoang, X. Lu, D. Niyato, P. Wang, and D. I. Kim, "Ambient backscatter communications: A contemporary survey," *IEEE Commun. Surveys Tuts.*, vol. 20, no. 4, pp. 2889–2922, 4th Quart., 2018.
- [15] B. Lyu, C. You, Z. Yang, and G. Gui, "The optimal control policy for RF-powered backscatter communication networks," *IEEE Trans. Veh. Technol.*, vol. 67, no. 3, pp. 2804–2808, Mar. 2018.
- [16] H. Guo, Y. Liang, R. Long, S. Xiao, and Q. Zhang, "Resource allocation for symbiotic radio system with fading channels," *IEEE Access*, vol. 7, pp. 34333–34347, 2019.
- [17] Q. Zhang, L. Zhang, Y. Liang, and P. Y. Kam, "Backscatter-NOMA: An integrated system of cellular and Internet-of-Things networks," in *Proc. IEEE Int. Conf. Commun. (ICC)*, 2019, pp. 1–6.
- [18] R. Long, H. Guo, and Y. Liang, "Symbiotic radio with full-duplex backscatter devices," in *Proc. IEEE Int. Conf. Commun. (ICC)*, 2019, pp. 1–6.
- [19] Z. Chu, W. Hao, P. Xiao, M. Khalily, and R. Tafazolli, "Resource allocations for symbiotic radio with finite blocklength backscatter link," *IEEE Internet Things J.*, vol. 7, no. 9, pp. 8192–8207, Sep. 2020.
- [20] X. Lu, D. Niyato, H. Jiang, D. I. Kim, Y. Xiao, and Z. Han, "Ambient backscatter assisted wireless powered communications," *IEEE Wireless Commun.*, vol. 25, no. 2, pp. 170–177, Apr. 2018.
- [21] Y. Ye, L. Shi, R. Q. Hu, and G. Lu, "Energy-efficient resource allocation for wirelessly powered backscatter communications," *IEEE Commun. Lett.*, vol. 23, no. 8, pp. 1418–1422, Aug. 2019.
- [22] D. Tse and P. Viswanath, *Fundamentals of Wireless Communication*. Cambridge, U.K.: Cambridge Univ. Press, 2005.
- [23] G. Yang, Q. Zhang, and Y.-C. Liang, "Cooperative ambient backscatter communications for green Internet-of-Things," *IEEE Internet Things J.*, vol. 5, no. 2, pp. 1116–1130, Apr. 2018.
- [24] Y. Xin, D. Wang, J. Li, H. Zhu, J. Wang, and X. You, "Area spectral efficiency and area energy efficiency of massive MIMO cellular systems," *IEEE Trans. Veh. Technol.*, vol. 65, no. 5, pp. 3243–3254, May 2016.
- [25] S. Guo, Y. Shi, Y. Yang, and B. Xiao, "Energy efficiency maximization in mobile wireless energy harvesting sensor networks," *IEEE Trans. Mobile Comput.*, vol. 17, no. 7, pp. 1524–1537, Jul. 2018.

[26] T. Liu, X. Qu, F. Yin, and Y. Chen, "Energy efficiency maximization for wirelessly powered sensor networks with energy beamforming," *IEEE Commun. Lett.*, vol. 23, no. 12, pp. 2311–2315, Dec. 2019.

[27] H. Zhang, M. Feng, K. Long, G. K. Karagiannidis, V. C. M. Leung, and H. V. Poor, "Energy efficient resource management in SWIPT enabled heterogeneous networks with NOMA," *IEEE Trans. Wireless Commun.*, vol. 19, no. 2, pp. 835–845, Feb. 2020.

[28] W. Dinkelbach, "On nonlinear fractional programming," *Manag. Sci.*, vol. 13, pp. 492–498, Mar. 1967. [Online]. Available: <http://www.jstor.org/stable/2627691>

[29] D. W. K. Ng, E. S. Lo, and R. Schober, "Energy-efficient resource allocation in OFDMA systems with large numbers of base station antennas," *IEEE Trans. Wireless Commun.*, vol. 11, no. 9, pp. 3292–3304, Sep. 2012.

[30] D. W. K. Ng, E. S. Lo, and R. Schober, "Wireless information and power transfer: Energy efficiency optimization in OFDMA systems," *IEEE Trans. Wireless Commun.*, vol. 12, no. 12, pp. 6352–6370, Dec. 2013.

[31] J. Gondzio and T. Terlaky, "A computational view of interior point methods," in *Advances in Linear and Integer Programming*(Oxford Lecture Series in Mathematics and its Applications), vol. 4, J. E. Beasley, Ed. Oxford, U.K.: Oxford Univ. Press, 1996, pp. 103–144.

[32] H. Zhang, C. Jiang, N. C. Beaulieu, X. Chu, X. Wen, and M. Tao, "Resource allocation in spectrum-sharing OFDMA femtocells with heterogeneous services," *IEEE Trans. Commun.*, vol. 62, no. 7, pp. 2366–2377, 2014.



KAI LIANG received the Ph.D. degree in information and communications engineering from Xidian University, China, in 2016, where he is a Lecturer with the State Key Laboratory of Integrated Service Networks. From September 2014 to September 2015, he was a visiting research student with the University of Essex, U.K., funded by the China Scholarships Council. His current research interests include network slicing, multiaccess edge computing, and wireless powered communications. He has co-organized two workshops at IEEE GLOBECOM 2019 and 2020.



research interests include wireless power transfer and backscatter communication network.

HAOHANG YANG received the B.Eng. degree from the Jinling Institute of Technology, Nanjing, China, and the De Montfort University, Leicester, U.K., in 2016, and the M.S. degree in wireless communication systems from the University of Sheffield, U.K., in 2017, where he is currently pursuing the Ph.D. degree. He attended the European commission decade project with Ranplan, Barcelona, Spain, in 2018. He has authored several technical articles in the IEEE transactions, journals, and letters. His current



transactions, journals, letters, and conferences. His research interests include cognitive radio networks, mobile edge computing, and wireless energy harvesting. He received the Exemplary Reviewer Award from the IEEE WIRELESS COMMUNICATIONS LETTERS in 2019. He served as a TPC Member for IEEE VTC-FALL 2019, IEEE ICCT 2019/2020/2021, and IEEE/CIC ICC 2021. He is also a Reviewer of multiple international journals, such as IEEE JOURNAL ON SELECTED AREAS IN COMMUNICATIONS, IEEE TRANSACTIONS ON COMMUNICATIONS, IEEE TRANSACTIONS ON WIRELESS COMMUNICATIONS, and IEEE TRANSACTIONS ON VEHICULAR TECHNOLOGY. He currently serves as an Editor for *Physical Communication* (Elsevier).

YINGHUI YE (Member, IEEE) received the Ph.D. degree in communication and information system from Xidian University in 2020. He was a joint Ph.D. student with the Department of Electrical and Computer Engineering, Utah State University, from 2018 to 2019. In 2020, he joined the Department of Communication and Information Engineering, Xi'an University of Posts and Telecommunications, where he is currently an Associate Professor. He has authored/coauthored more than thirty technical articles in the IEEE



XIAOLI CHU (Senior Member, IEEE) received the B.Eng. degree in electronic and information engineering from Xi'an Jiao Tong University in 2001 and the Ph.D. degree in electrical and electronic engineering from the Hong Kong University of Science and Technology in 2005. She is a Professor with the Department of Electronic and Electrical Engineering, University of Sheffield, U.K. From 2005 to 2012, she was with the Centre for Telecommunications Research, King's College London. She has coauthored over 150 peer-reviewed journal and conference papers. She coauthored/co-edited the books *Fog-Enabled Intelligent IoT Systems* (Springer, 2020), *Ultra Dense Networks for 5G and Beyond* (Wiley, 2019), *Heterogeneous Cellular Networks: Theory, Simulation and Deployment* (Cambridge University Press, 2013), and *4G Femtocells: Resource Allocation and Interference Management* (Springer, 2013). She is co-recipient of the IEEE Communications Society 2017 Young Author Best Paper Award. She received the IEEE COMMUNICATIONS LETTERS Exemplary Editor Award in 2018. She was Co-Chair of Wireless Communications Symposium for IEEE ICC 2015, a Workshop Co-Chair for IEEE GreenCom 2013, and has co-organized eight workshops at IEEE ICC, GLOBECOM, WCNC, and PIMRC. She is Senior Editor for the IEEE WIRELESS COMMUNICATIONS LETTERS and an Editor for the IEEE COMMUNICATIONS LETTERS.